

Sb-induced bulk band transitions in Si(111) and Si(001) observed in synchrotron photoemission studies

D. H. Rich, T. Miller, G. E. Franklin, and T.-C. Chiang

*Department of Physics and Materials Research Laboratory, University of Illinois at Urbana-Champaign,
1110 W. Green Street, Urbana, Illinois 61801*

(Received 3 October 1988)

The Sb saturation of Si(111) and Si(001) was found by angle-resolved photoemission to allow the measurement of the bulk band-dispersion relations along the high-symmetry Γ - Λ - L and Γ - Δ - X directions over a wide photon-energy range. Core-level spectroscopy revealed that the Si atoms in the near-surface region are converted to exhibit a bulklike atomic arrangement after Sb coverage. Strain reduction mechanisms in the near-surface region are addressed.

We present an application of angle-resolved photoemission spectroscopy and molecular-beam epitaxy (MBE) to a measurement of the Si bulk valence-band structure along the [111] (Γ - Λ - L) and [001] (Γ - Δ - X) high-symmetry directions. The photoemission technique has proven to be a valuable tool for mapping the bulk band structure of important semiconductors such as GaAs and Ge.¹⁻⁴ However, previous attempts at obtaining the bulk band dispersions of Si have produced only very limited success. Using a normal-emission method, bulk band transitions from the valence bands to the free-electron-like final band were observed over a small part of the band structure for the Si(001)-(2 \times 1) surface, while no discernible dispersion was observed for the Si(111)-(7 \times 7) surface.⁴ The present experiment demonstrates that by terminating the Si(111) and Si(001) surfaces with Sb, previously unobserved bulk band-dispersion relations along the Γ - Λ - L and Γ - Δ - X directions are now observed over a wide photon energy range, allowing for a more complete mapping of the Si band structure. Core-level spectroscopy of the Si 2*p* level and high-energy electron diffraction (HEED) are also employed to assess the effects of the Sb termination on the surface electronic and atomic structure. In general, fundamental studies of the interaction between various group V adsorbates with the Si surfaces are motivated by the current industrial interest for incorporating group III-V materials with the well-developed Si technology.

The photoemission experiments were carried out with synchrotron radiation dispersed by a 6-m toroidal-grating monochromator on the 1-GeV storage ring at the Synchrotron Radiation Center of the University of Wisconsin-Madison at Stoughton, Wisconsin. A hemispherical analyzer having a full acceptance angle of 3° was employed for the normal-emission experiments, while an angle-integrating hemispherical analyzer was used for the core-level measurements. The overall instrumental resolution was 100–200 meV. The Fermi-level position was determined by observing the Fermi-edge emission of a gold foil in electrical contact with the sample. The HEED measurements and MBE growth were performed in the same vacuum chamber. The *n*-type Si(111) and Si(001) samples were cleaned by thermal annealing at 1100 and 1250°C, respectively, for 10 s. The Sb overlayers were

prepared by evaporation with a rate of 3–10 monolayers (ML) per minute. In this paper 1 ML of Sb is defined as the site density for the unreconstructed surface in question, which is 6.8×10^{14} and 7.8×10^{14} atoms/cm² for Si(001) and Si(111), respectively. The sample temperature during evaporation was maintained within 320–370°C, and typical Sb exposures ranged from 30 to 50 ML. Upon exposure to the Sb beam, the sticking coefficient was found to approach zero once the surface

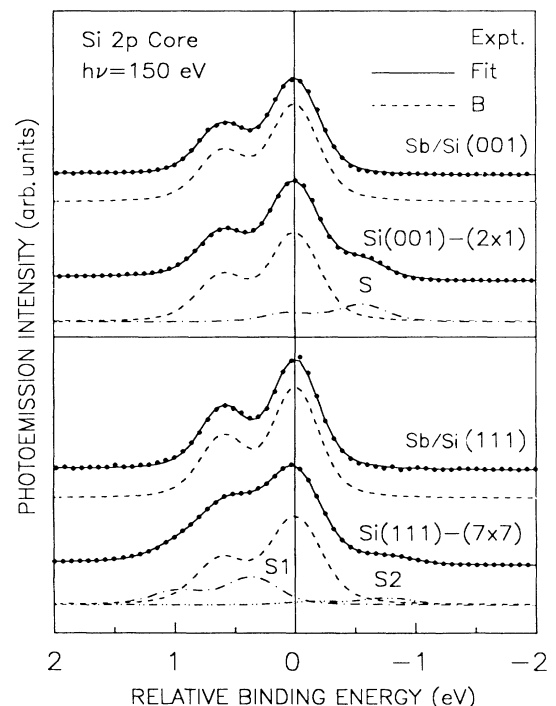


FIG. 1. Si 2*p* core-level spectra taken with a photon energy of 150 eV for the Si(111)-(7 \times 7), Si(001)-(2 \times 1), and Sb-saturated surfaces. The solid curves running through the data points (dots) are fits to the data. The other curves show the decomposition into bulk (*B*) and surface (*S*, *S*₁, and *S*₂) contributions. The binding energy is referred to the bulk Si 2*p*_{3/2} components.

coverage approached the saturation limit of approximately 1 ML,⁵⁻⁷ and the HEED results indicated that both systems transformed into a (1×1) surface at saturation. The photoemission measurements were performed with the sample at nearly room temperature.

The Si 2*p* core-level spectra (filled circles) are shown in Fig. 1 for both the clean and Sb-saturated surfaces. Previous studies of the clean surfaces employing a nonlinear least-squares-fitting procedure have shown that the line shapes contain surface and bulk contributions; the details of this analysis can be found in earlier publications.⁸⁻¹⁰ The Si(111)-(7×7) spectrum shows two surface components (labeled *S*1 and *S*2) in addition to the bulk component (labeled *B*), while the spectrum for the Si(001)-(2×1) surface shows one surface component (labeled *S*). These surface-shifted components have been related to specific details of the reconstruction.^{8,10} With Sb coverage, the surface shifts are suppressed, and the core-level spectra in Fig. 1 are seen to convert to exhibit a single bulklike component. The simplest interpretation is that the adsorption of Sb causes all dangling bonds on the Si

surfaces to become saturated and results in a bulklike fourfold bonding arrangement for the Si surface atoms. This behavior is similar to other covalently bonded adsorbate systems such as In/Si(001),⁹ Sn/Si(001),¹¹ and Ge/Si(111).⁸ In addition to suppressing the surface components, Sb coverage causes the bulk core-level component to shift relative to the Fermi level, which is the well-known band-bending effect. From the known Fermi-level position within the band gap for the clean surface and the measured change in band bending, the position of the valence-band maximum relative to the Fermi level was determined for each Sb-covered surface.⁷

The angle-resolved normal-emission spectra for the clean Si(111)-(7×7) and Si(001)-(2×1) surfaces are shown at the bottoms of Figs. 2 and 3, respectively, and are consistent with previous measurements.^{4,12,13} The surface states in the Si(111)-(7×7) spectrum are labeled *T*1, *T*2, and *T*3 and have been previously identified from scanning tunneling microscopy (STM) as being derived from the adatom dangling bonds, restatom dangling bonds, and adatom back bonds, respectively.^{8,14} The

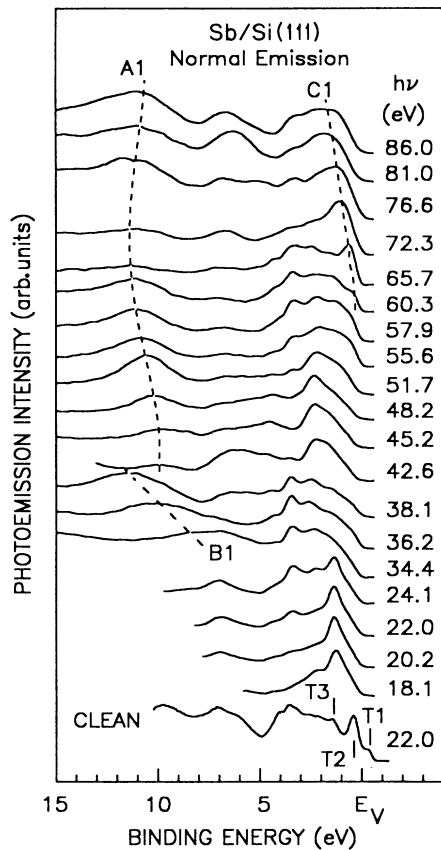


FIG. 2. Normal-emission spectra for the Si(111)-(7×7) and Sb-saturated Si(111) surfaces taken with the indicated photon energies. The binding energy is referred to the valence-band maximum (E_V). Dispersive peaks are indicated by the dashed curves and labeled for clarity. The clean Si(111)-(7×7) spectrum is shown at the bottom for $h\nu=22.0$ eV; various surface states are indicated by the labels *T*1, *T*2, and *T*3.

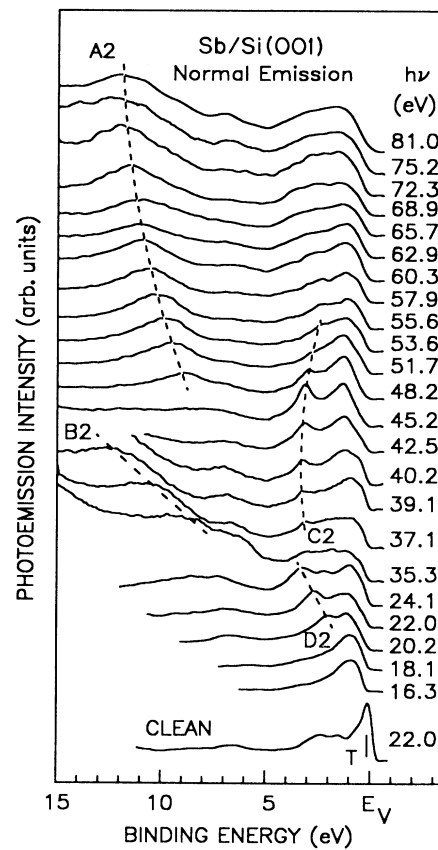


FIG. 3. Normal-emission spectra for the Si(001)-(2×1) and Sb-saturated Si(001) surfaces taken with the indicated photon energies. The binding energy is referred to the valence-band maximum (E_V). Dispersive peaks are indicated by the dashed curves and labeled for clarity. The clean Si(001)-(2×1) spectrum is shown at the bottom for $h\nu=22.0$ eV; the surface state is indicated by the label *T*.

Si(001)-(2×1) spectrum contains a strong surface-state feature labeled T , and STM shows that it originates from the dimer dangling bonds.¹⁵ At Sb saturation, the surface states are no longer present. This is consistent with the core-level findings which indicate that all Si surface dangling bonds are saturated by Sb adsorption.

The normal-emission spectra for the Sb-saturated Si(111) and Si(001) surfaces are shown for various photon energies in Figs. 2 and 3, respectively. Several non-dispersive emission features are apparent. These peaks may be derived from critical points associated with the one-dimensional density of states, from three-dimensional density-of-states features, or from Sb-induced surface or interface states. Their assignment based on the present experiment is uncertain and the emphasis here will be on the dispersive features. Peaks $B1$ and $B2$ have a nearly constant kinetic energy and are derived from the Sb NVV Auger transition. The other dispersive peaks $A1$, $C1$, $A2$, $C2$, and $D2$ can be identified as direct transitions from the bulk Si valence bands. Only peaks $C2$ and $D2$ have been previously observed for the case of Si(001)-(2×1),⁴ while $A1$, $C1$, and $A2$ have not been previously observed.

The technique of k_{\perp} band mapping has been discussed in detail for the GaAs and Ge surfaces,¹⁻³ and the assignment of the present dispersive peaks are facilitated by comparison with these studies. The theoretical valence-band dispersions of Si along the Γ - Δ - X and Γ - Λ - L directions obtained by Chelikowsky and Cohen using a local pseudopotential (dashed curve) and a nonlocal pseudopotential (solid curve) method are displayed in Fig. 4.¹⁶ Peaks $C1$ and $C2$ are assigned as direct transitions from the uppermost valence band, while peaks $A1$ and $A2$ are assigned as direct transitions from the lowest valence band (the s -like band). The final-state band in this model is approximated by a free-electron dispersion relation, assuming an inner potential of 5.6 eV referred to the valence-band maximum.^{4,7,17,18} This free-electron approximation is good only for relatively high photon energies ($h\nu \gtrsim 30$ eV); therefore, it is not applicable for peak $D2$ as discussed previously.⁴ The resulting band dispersions from the Sb-saturated Si(111) and Si(001) surfaces are indicated in Fig. 4 by filled circles and squares, respectively. The open circles represent the data obtained from clean Si(001)-(2×1) reported previously.⁴ The typical energy error shown in Fig. 4 reflects the uncertainty in peak-position determination; the typical momentum error is mainly due to the uncertainty in the inner potential and the broadening of the free-electron final band by crystal-potential and lifetime effects. Allowing for the errors, the agreement between experiment and theory is generally good. The most significant differences are in the binding energies of the L_3' and X_1 critical points; the theory puts these two points too high.

The absence of dispersive bulk band transitions from the clean Si(111)-(7×7) and Si(001)-(2×1) systems under similar experimental conditions was speculated to be caused by surface strain and reconstruction, and the resulting crystal-lattice distortion was argued to extend at least on the order of the photoelectron escape depth of Si (5 to 7 Å).⁴ Since the Sb termination is found to suppress the reconstructions and to saturate all surface dangling

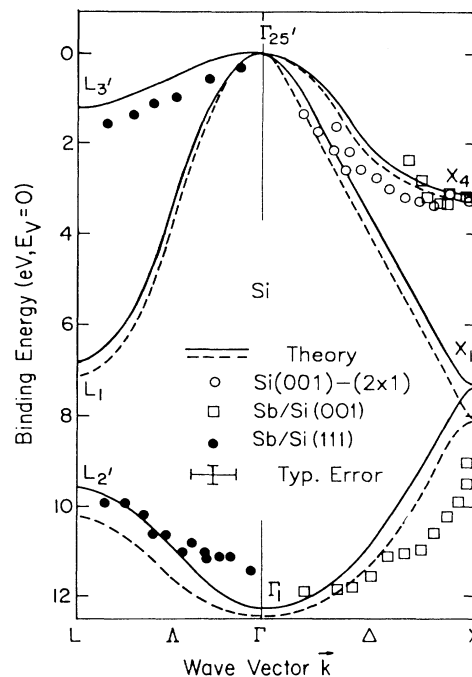


FIG. 4. Bulk valence-band structure of Si along the Γ - Λ - L and Γ - Δ - X directions. The solid and dashed curves are theoretical calculations from a nonlocal and local pseudopotential calculation, respectively, from Ref. 16. The open circles are data from Ref. 4. The filled circles and squares are data obtained from bulk band dispersions on the Sb-saturated Si(111) and Si(001) surfaces, respectively.

bonds, the Sb-induced bulk band transitions observed here are possibly due to a reduction in lattice distortion caused by adsorbate-to-substrate bonding. There exists other evidence in the literature that adsorbates can modify the surface strain. Uhrberg, Bringans, Olmstead, and Bachrach, using a constant photon energy of 21.2 eV and off-normal ($k_{\parallel} \neq 0$) scans, demonstrated that the As termination of Si(111) sharpens certain existing peaks in the valence-band spectra.¹⁹ Low-energy electron diffraction results also show that adsorbates can reduce the surface relaxation for a variety of metal surfaces.²⁰

In conclusion, core-level spectroscopy has shown that the Sb termination of Si(111) and Si(001) removes all surface-shifted components resulting in a bulklike atomic environment for the outermost Si layers. The Sb termination is found to cause the appearance of bulk-band-derived dispersive peaks in the normal-emission spectra over a wide photon energy range which were previously unobserved for the clean Si(111)-(7×7) and Si(001)-(2×1) surfaces. The bulk band dispersions have been mapped over a wide momentum range along the Γ - Λ - L and Γ - Δ - X high-symmetry directions and are compared with the theoretical calculations of Chelikowsky and Cohen. The present results strongly suggest that the Sb termination causes a reduction in strain for the outermost Si layers on Si(111) and Si(001).

This material is based upon the work supported by the U.S. Department of Energy (DOE), Division of Materials Sciences, under Contract No. DE-AC02-76ER01198. Some of the personnel and equipment support was also derived from grants from the National Science Foundation (NSF) (Grants No. DMR-8352083 and No. DMR-8614234), the IBM T. J. Watson Research Center (Yorktown Heights, NY), and the E. I. du Pont de Nemours and Company (Wilmington, DE). The Synchrotron Radi-

ation Center of the University of Wisconsin-Madison is supported by the NSF under Contract No. DMR-8020164. We acknowledge the use of central facilities of the Materials Research Laboratory of the University of Illinois, which is supported by the U.S. DOE, Division of Materials Sciences, under Contract No. DE-AC02-76ER01198, and the NSF under Contract No. DMR-8612860.

-
- ¹T.-C. Chiang, J. A. Knapp, M. Aono, and D. E. Eastman, *Phys. Rev. B* **21**, 3513 (1980).
- ²T.-C. Chiang, R. Ludeke, M. Aono, G. Landgren, F. J. Himpsel, and D. E. Eastman, *Phys. Rev. B* **27**, 4770 (1983).
- ³T.-C. Hsieh, T. Miller, and T.-C. Chiang, *Phys. Rev. B* **30**, 7005 (1984).
- ⁴A. L. Wachs, T. Miller, T. C. Hsieh, A. P. Shapiro, and T.-C. Chiang, *Phys. Rev. B* **32**, 2326 (1985).
- ⁵R. A. Metzger and F. G. Allen, *J. Appl. Phys.* **55**, 931 (1984).
- ⁶S. A. Barnett, H. F. Winters, and J. E. Greene, *Surf. Sci.* **165**, 303 (1986).
- ⁷D. H. Rich, A. Samsavar, T. Miller, F. M. Leibsle, and T.-C. Chiang (unpublished).
- ⁸T. Miller, T. C. Hsieh, and T.-C. Chiang, *Phys. Rev. B* **33**, 6983 (1986).
- ⁹D. H. Rich, A. Samsavar, T. Miller, H. F. Lin, T.-C. Chiang, J.-E. Sundgren, and J. E. Greene, *Phys. Rev. Lett.* **58**, 579 (1987).
- ¹⁰D. H. Rich, T. Miller, and T.-C. Chiang, *Phys. Rev. B* **37**, 3124 (1988), and references therein.
- ¹¹D. H. Rich, T. Miller, A. Samsavar, H. F. Lin, and T.-C. Chiang, *Phys. Rev. B* **37**, 10221 (1988).
- ¹²J. E. Demuth, B. N. J. Parsson, and A. J. Schell-Sorokin, *Phys. Rev. Lett.* **51**, 2214 (1983), and references therein.
- ¹³F. J. Himpsel and D. E. Eastman, *J. Vac. Sci. Technol.* **16**, 1297 (1979).
- ¹⁴R. J. Hamers, R. M. Tromp, and J. E. Demuth, *Phys. Rev. Lett.* **56**, 1972 (1986); *Surf. Sci.* **181**, 346 (1987).
- ¹⁵R. J. Hamers, Ph. Avouris, and F. Bozso, *J. Vac. Sci. Technol. A* **6**, 508 (1988).
- ¹⁶J. R. Chelikowsky and M. L. Cohen, *Phys. Rev. B* **14**, 556 (1976).
- ¹⁷S. Y. Tong, H. Huang, C. M. Wei, W. E. Packard, F. K. Men, G. Glander, and M. B. Webb, *J. Vac. Sci. Technol. A* **6**, 615 (1988).
- ¹⁸The inner potential used here has been determined from a separate study in Ref. 7 and is close to the values used in Ref. 4 (4.2 eV with respect to the Fermi level) and Ref. 17 (~10 eV with respect to the vacuum level) when adjusting for the different energy references.
- ¹⁹R. I. G. Uhrberg, R. D. Bringans, M. A. Olmstead, and R. Z. Bachrach, *Phys. Rev. B* **35**, 3945 (1987).
- ²⁰A. P. Baddorf, I.-W. Lyo, E. W. Plummer, and H. L. Davis, *J. Vac. Sci. Technol. A* **5**, 782 (1987).